

# Magnetic behavior and role of the antiphase boundaries in Fe<sub>3</sub>O<sub>4</sub> epitaxial films sputtered on MgO (001)

J.F. Bobo<sup>1,a</sup>, D. Basso<sup>1</sup>, E. Snoeck<sup>2</sup>, C. Gatel<sup>2</sup>, D. Hrabovsky<sup>1</sup>, J.L. Gauffier<sup>1</sup>, L. Ressier<sup>1</sup>, R. Mamy<sup>1</sup>, S. Visnovsky<sup>4</sup>, J. Hamrle<sup>4</sup>, J. Teillet<sup>3</sup>, and A.R. Fert<sup>1</sup>

<sup>1</sup> Laboratoire de Physique de la Matière Condensée<sup>b</sup>, 135 avenue de Rangueil, 31077 Toulouse Cedex 4, France

<sup>2</sup> CEMES CNRS, 29 rue Jeanne Marvig, 31055 Toulouse Cedex 4, France

<sup>3</sup> Groupe de Physique des Matériaux<sup>c</sup>, Faculté des Sciences de Rouen, 76821 Mont Saint Aignan Cedex, France

<sup>4</sup> Faculty of Mathematics and Physics, Charles University, Ke Karlovu 3, 121 16 Prague 2, Czech Republic

Received 2 July 2001

**Abstract.** Magnetite Fe<sub>3</sub>O<sub>4</sub> films were grown on single crystal MgO (001) substrates using facing target sputtering technique. Conversion Electron Mössbauer Spectroscopy and magneto optical polar Kerr spectra have confirmed the stoichiometric repartition of Fe cations corresponding to the inverse spinel structure and the electronic structure characteristic of bulk Fe<sub>3</sub>O<sub>4</sub>. Hysteresis loops carried out at room temperature show that, in a 1 T applied magnetic field, only 60% of the saturation magnetization is detected. This behavior is discussed in correlation to the antiphase boundaries (APBs) observed by electron microscopy. Magnetic force microscopy studies show that magnetic domains are larger than the mean distance between APBs.

**PACS.** 75.70.-i Magnetic properties of thin films, surfaces, and interfaces – 75.60.-d Domain effects, magnetization curves, and hysteresis – 78.20.Ls Magneto-optical effects

## 1 Introduction

The spin dependent transport has generated a lot of work in order to grow magnetic oxide layers exhibiting high degree of spin polarization. Clearly first candidate for this type of system was obtained with mixed valence manganites which were extensively studied for colossal magnetoresistance phenomena. In particular La<sub>0.7</sub>Sr<sub>0.3</sub>MnO<sub>3</sub> appears to be a ferromagnetic oxide with only one spin direction at the Fermi level and can be considered as a half-metallic compound [1]. Unfortunately La<sub>0.7</sub>Sr<sub>0.3</sub>MnO<sub>3</sub> has a relatively low Curie temperature ( $T_c \sim 360$  K) incompatible with magnetic tunnel junctions (MTJ) applications at room temperature. More recently, double perovskites as Sr<sub>2</sub>FeMoO<sub>6</sub> [2] appear promising because of their higher Curie temperature ( $T_c \sim 400$  K). The Fe<sub>3</sub>O<sub>4</sub> magnetite is a well known magnetic oxide material with a good potential for applications considering its high Curie temperature  $T_c \sim 850$  K [3]. Most of the recent studies show that electrical conductivity in thin layers is small compared to bulk samples and that conductivity is associated to hopping of minority spins electrons between octahedral Fe sites of the Fe<sub>3</sub>O<sub>4</sub> spinel structure. According to Zhang *et al.* [4] calculus, for  $T > T_V$  ( $T_V$  is the Verwey transition temperature), in octahedral sites, only spins up

electrons are present at the Fermi level. This result predicts a half metallic behavior at room temperature [4,5]. Several research groups [6–10] have tested this type of oxide for spin polarized transport system. An important work has been realized by Margulies *et al.* [11] on Fe<sub>3</sub>O<sub>4</sub> films deposited on MgO substrates by various methods (sputter deposition, molecular beam epitaxy and evaporation); the authors show that magnetization deviates from bulk single crystal behavior and exhibits large saturation fields and quasi random zero field magnetic moment distribution. In a second paper [12] Margulies *et al.* propose that this behavior results from the antiphase boundaries (APBs) which are present in Fe<sub>3</sub>O<sub>4</sub> films.

In this paper letter we report on the growth of epitaxial Fe<sub>3</sub>O<sub>4</sub> layers on MgO single crystal substrates, analysis of the structure of the deposited layer was done by RHEED *in situ*, X-ray diffraction and Transmission Electron Microscopy (TEM). We present Mössbauer, SQUID and magneto optical study of the magnetic properties. TEM observations of antiphase boundaries, Magnetic Force Microscopy (MFM) study of magnetic domains allow us to achieve an interpretation of the magnetic behavior.

## 2 Samples preparation and structural properties

The magnetite Fe<sub>3</sub>O<sub>4</sub> layers have been grown on single crystal MgO (001) substrates using facing target sputter

---

<sup>a</sup> e-mail: bobo@insa-tlse.fr

<sup>b</sup> UMR 5830 UPS-CNRS-INSA

<sup>c</sup> UMR CNRS 6634

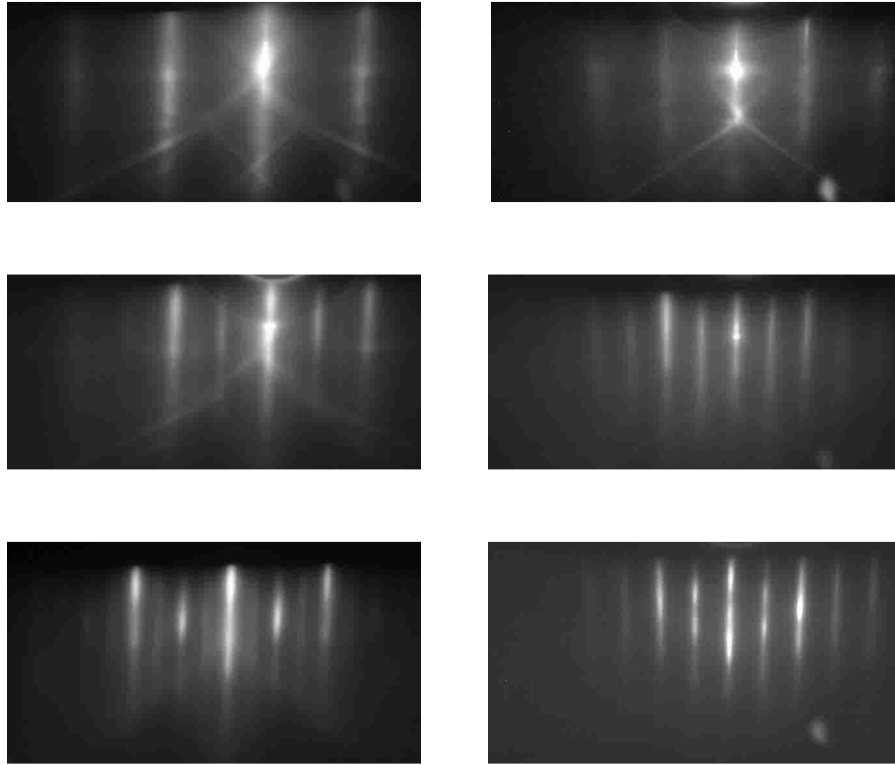


**Fig. 1.** RHEED patterns collected along (100) and (110) azimuths for respectively a bare MgO substrate ((a) and (b)), a 190 Å thick  $\text{Fe}_3\text{O}_4$  film ((c) and (d)) and a 1875 Å thick  $\text{Fe}_3\text{O}_4$  film ((e) and (f)).

technique [13] with a UHV chamber.  $\text{Fe}_2\text{O}_3$  ceramics are placed on rf-polarized face-to-face cathodes. The chemical homogeneity and stoichiometry of the targets and films were checked by electron microprobe analysis. Deposition was performed in a pure argon plasma and the best epitaxial quality was obtained for a substrate temperature of  $\sim 400^\circ\text{C}$ . The magnetite crystallizes in the fcc structure (space group Fd-3m) with a lattice parameter  $a = 8.39 \text{ \AA}$  which is twice larger than the parameter of fcc MgO ( $a_{\text{MgO}} = 4.21 \text{ \AA}$ ). The oxygen atoms lie in the  $\{200\}_{\text{MgO}}$  and  $\{400\}_{\text{Fe}_3\text{O}_4}$  planes. Since the misfit between these planes is  $\sim 0.3\%$ , epitaxial growth of magnetite on MgO is achievable. A set of samples, deposited in the same conditions, has been realized with thickness ranging from 95 Å to 1875 Å. The thicker sample was dedicated to Conversion Electron Mössbauer Spectroscopy (CEMS).

Reflection High Energy Electron Diffraction (RHEED) measurements were performed before and after film growth with accurate substrate positioning and along several azimuths. Figure 1 shows typical RHEED patterns with lattice rods demonstrating epitaxial quality of the films and good matching of  $\text{Fe}_3\text{O}_4$  crystal on MgO (001). The appearance of additional rods between the direct beam and the MgO (100) and MgO (110) reflexions is the signature of the  $\text{Fe}_3\text{O}_4$  unit cell. Quantitative RHEED pattern analysis yields a value of  $a(\text{Fe}_3\text{O}_4) = 8.4 \pm 0.1 \text{ \AA}$  for all films.

Structural characterizations of the magnetite thin films were performed by Transmission Electron Microscopy

(TEM) both in plane view and cross sectional specimens. The specimens were thinned to the electron transparency by the usual method and the experiments were carried out on a Philips CM30 whose point resolution is 1.9 Å. High Resolution TEM (HRTEM) analyses performed on the cross sectional specimens give evidence of the pseudomorphic growth of  $\text{Fe}_3\text{O}_4$  on MgO (001) as it is presented in the micrograph and the corresponding diffraction pattern in Figure 2. In the latter the 020 MgO type reflections are superimposed with the 040  $\text{Fe}_3\text{O}_4$  type spots evidencing the lattice relationship:  $\text{Fe}_3\text{O}_4 (001)[100]//\text{MgO} (001)[100]$ . The HRTEM micrograph of the  $\text{Fe}_3\text{O}_4/\text{MgO}$  interface in Figure 2 confirms the epitaxial growth of the magnetite on MgO (001). No inter-phase was evidenced at the  $\text{Fe}_3\text{O}_4/\text{MgO}$  interface and a misfit dislocation is pointed out in Figure 2 with its corresponding Burger circuit. To get a complete plastic relaxation of the magnetite thin film on MgO (001) the dislocation network should have a mean periodicity of 700 Å.

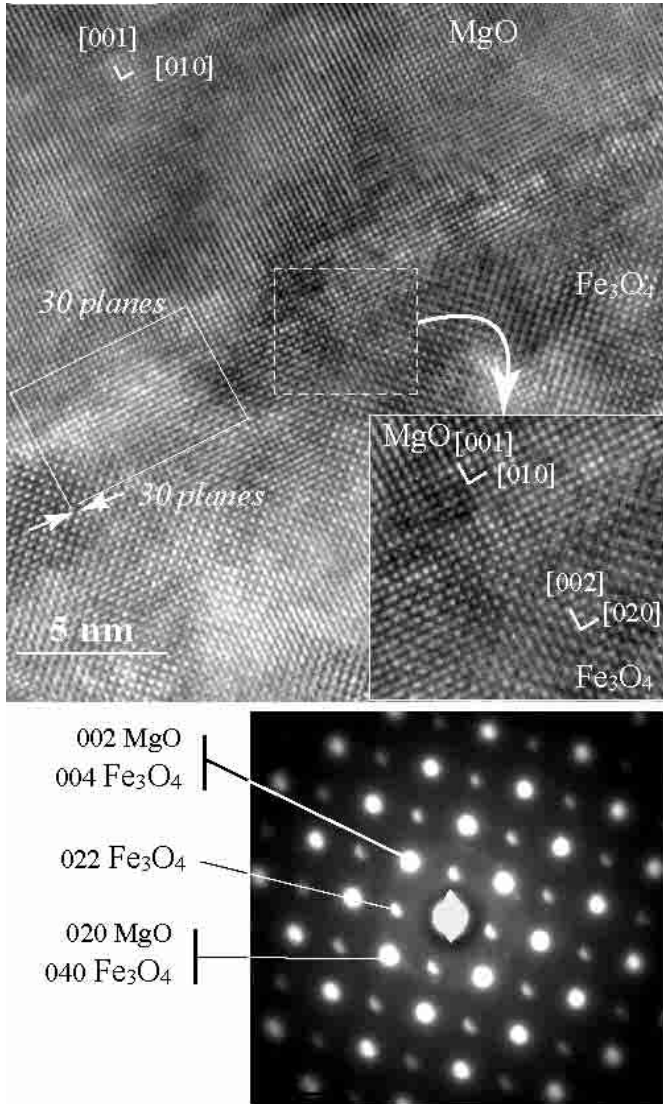
### 3 Magnetic properties

#### 3.1 Mössbauer spectroscopy

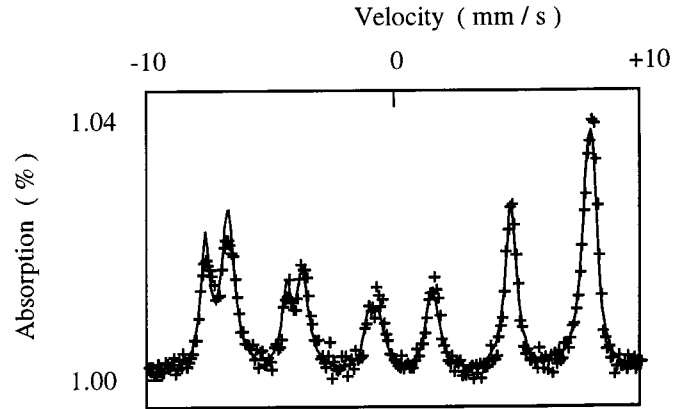
CEMS spectrum presented in Figure 3 is observed at room temperature and zero magnetic field on 1875 Å thick sample. It can be fitted with only two sextets. The result of fitting is reported in Table 1. It is in agreement

**Table 1.** Room temperature hyperfine parameters of components. IS: isomer shift relative to  $\alpha$  iron at room temperature,  $B_{\text{hf}}$ : hyperfine field;  $2\varepsilon$ : quadrupolar shift.

component	IS(mm s <sup>-1</sup> )	2 $\varepsilon$ (mm s <sup>-1</sup> )	$B_{\text{hf}}$ (T)	abundance (%)
A-site	0.30 $\pm$ 0.01	0.004 $\pm$ 0.004	49.1 $\pm$ 0.2	36
B-site	0.63 $\pm$ 0.01	0.038 $\pm$ 0.004	45.6 $\pm$ 0.2	64

**Fig. 2.** HRTEM micrograph of a 750 Å thick Fe<sub>3</sub>O<sub>4</sub> film deposited on MgO (001) with its corresponding diffraction pattern inset. Both the image and the diffraction evidences the epitaxial growth of the magnetite.

with a tetrahedral A and octahedral B site iron species with a relative occupancy in the ratio close to the theoretical value of 0.5. In bulk Fe<sub>3</sub>O<sub>4</sub> inverse spinel, A sites contain only Fe<sup>3+</sup> ions and the B sites contain equal numbers of Fe<sup>2+</sup> and Fe<sup>3+</sup> ions. This distribution is also present in our Fe<sub>3</sub>O<sub>4</sub> films as could be shown first on the isomer shift 0.63 mm/s on site B and 0.30 mm/s on site

**Fig. 3.** Mössbauer spectrum at zero magnetic field and room temperature for a 187 Å thick magnetite film. Crosses are experimental points and solid line is fitted curve corresponding to hyperfine parameters presented in Table 1.

A. The observed electric field gradient on site A (cubic symmetry) is zero. For this site, this is in agreement with Fe<sup>3+</sup> ions, which have spherical symmetry, resulting of the S electronic configuration. Moreover, the hyperfine fields on sites A and B appear clearly proportional to mean magnetic moments on site A ( $5\mu_B$ ) and B ( $(5+4)/2\mu_B$ ). The relative intensity of the lines in each sextet depends directly on the angle between magnetic moments and  $\gamma$ -ray direction which is perpendicular to the plane of the film. We observe for both Mössbauer spectra a mean angle of  $52^\circ$  which is very close to what is found for random orientation ( $54.7^\circ$ ) demonstrating a quasi 3D-random magnetic moment distribution. So Mössbauer experiments conduct to a zero-magnetic field random orientation of the various magnetic domains of the Fe<sub>3</sub>O<sub>4</sub> layer in spite of shape anisotropy, as was previously observed by Margulies *et al.* [11].

### 3.2 Magneto optical properties

Use of magneto optical technique for probing the magnetic behavior of thin films is appropriate due to the absence of substrate contribution. Moreover room temperature measurements are convenient, sample can be easily oriented in the air coil and, with a 50 Hz alternative magnetic field and the use of a fast AD converter a complete hysteresis cycle can be obtained in 20 ms. By this way a large number of hysteresis cycles have been realized to study at first the in-plane magnetic behavior. We observe for all samples that in plane anisotropy is very small, numerous

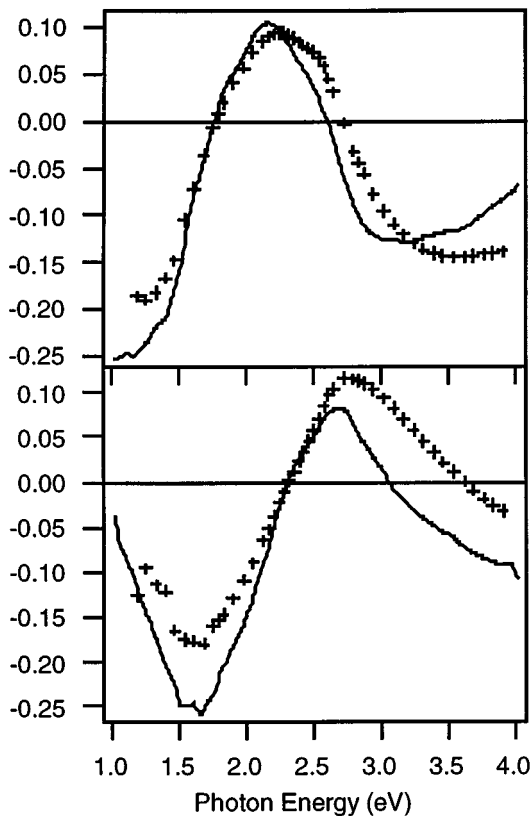


**Fig. 4.** Kerr rotation and ellipticity *vs.* photon energy for a 280 Å thick  $\text{Fe}_3\text{O}_4$  film. Crosses are experimental results, dashed lines are the fits.

hysteresis loops being collected for various azimuthal angles in the film plane. This result confirms the small value of the magnetocrystalline anisotropy as noticed in bulk samples  $K \approx -1.1 \times 10^5 \text{ erg/cm}^3$  [3] and that our deposition procedure does not induce any anisotropic term. The coercive field observed is always close to 300 Oe, value reported for bulk  $\text{Fe}_3\text{O}_4$ . It clearly appears that, for the field range corresponding to results obtained by magneto optical technique ( $H$  maximum being 2 T) the observed magnetization loops do not reach saturation since there is a residual slope above 1000 Oe. This result will be confirmed by our SQUID measurements. Moreover, we have not observed the appearance of a bias field or exchange field which could be correlated to the presence in our films of antiferromagnetic oxide of FeO type. This oxide could be present in case of higher temperature deposition ( $T > 400^\circ\text{C}$ ).

The polar Kerr spectroscopy was carried out with external magnetic field of 1.33 T which is sufficient to ensure the first step and main magnetic saturation of our samples but we cannot exclude the presence of domains pinned by exchange coupling with antiparallel magnetization direction as previously proposed. The polar Kerr rotation and Kerr ellipticity energy dependence of a 280 Å film are displayed in Figure 4. In this figure we could compare experimental results and results obtained by a modeling

calculus taking into account the bulk  $\text{Fe}_3\text{O}_4$  dielectric tensor elements and their spectral dependence from the paper work of Fontijn *et al.* [14,15], where diagonal elements are obtained from spectroscopic ellipsometry measurements and where off diagonal elements are derived from measured polar Kerr spectrum. We observe a good agreement between experimental and calculated results, the shapes of the two curves presented are very similar, the photon energy dependence is associated to Inter-Valence Charge Transfer (IVCT) transitions (transitions in which an electron, through optical excitation, is transferred to a neighboring cation) and is clearly characteristic of  $\text{Fe}_3\text{O}_4$  compound, demonstrating one more time the presence of single phase magnetite in our films, strongly suggestive of half metallic behavior. However the amplitude of the Kerr rotation and ellipticity obtained by calculus and by measurements slightly differ. This could be understood by two ways, at first the magnetization is not saturated and misaligned domains give an opposite contribution to the Kerr rotation, moreover we have considered for the calculus an infinite MgO substrate. Experimental data correspond to finite substrate thickness with rough back face. In that case, it is impossible to take into account light reflection and scattering on the back of the substrate.

### 3.3 Bulk magnetization measurements

SQUID measurements allow us to estimate the value of the magnetization up to 5 T, and to compare it to the bulk saturation magnetization. Results obtained at room temperature for several samples with different thickness, and for in plane magnetic field, are presented Figure 5. We could observe, as was noticed for magneto optical measurements, that saturation seems to be reached at 1 T, but with a residual slope extending to larger magnetic fields. SQUID measurements performed up to 5 T do not reach the bulk saturation value of  $480 \text{ emu/cm}^3$  [3]. This is indicative of the presence of antiferromagnetically exchange-coupled domains through APB's defects. For most of the samples, at 1 tesla, the magnetization is roughly equal to 60% of the bulk value. These results are in agreement with results of Margulies *et al.* [11] and Seneor *et al.* [6].

For magnetic field perpendicular to the plane of the sample, the magnetization reaches its maximum value for larger fields than for in plane configuration, essentially due to shape anisotropy which correspond to a field of roughly 6 kOe ( $4\pi M_S$ ). As observed with in-plane magnetic field, the value of saturation magnetization is roughly 60% of the bulk value. These results are coherent with the hypothesis of ferromagnetic domains limited by APBs introducing random orientation of the magnetization in zero magnetic field. In a first step most of the domains are reoriented in the field direction but some APBs induce an antiparallel ordering between neighboring domains and this explains why in a one tesla magnetic field the global magnetization is reversed but 20% of the domains are pinned in opposite direction.

We could observe that for the thinnest magnetite film, hysteresis loops are no longer open as well as there is

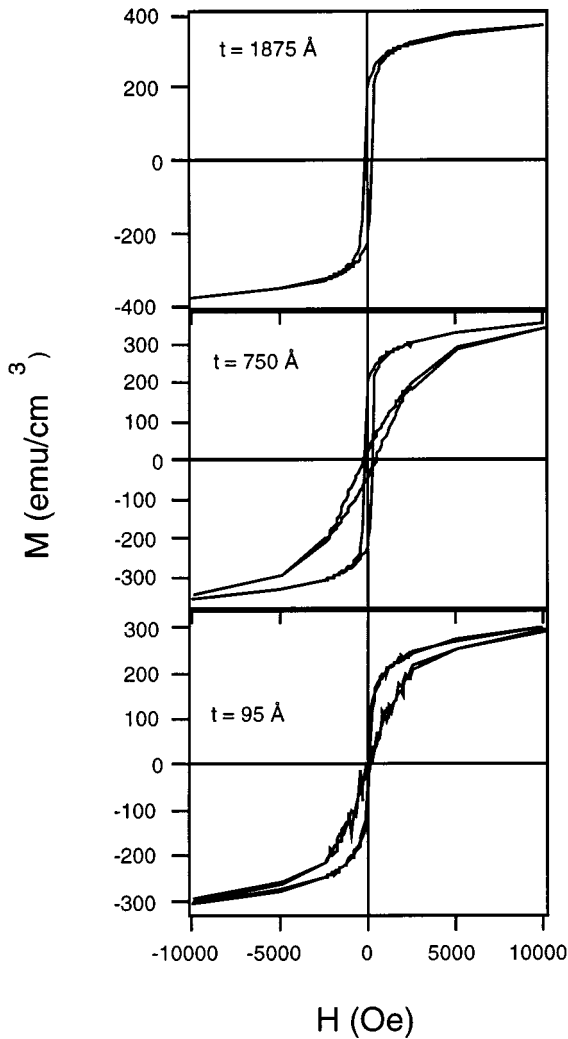


**Fig. 5.** SQUID measurements (in plane: solid line, out-of-plane: broken line) for three different thickness of Fe<sub>3</sub>O<sub>4</sub> films.

no more remanent magnetization. This is indicative of a loss of irreversibility processes in the magnetic switching. These results could be interpreted in terms of an increase of the APBs density related to surface defects. APBs induce a complete disorder of domain magnetization for the thinnest films. For the same reason, the saturation magnetization at 5 T is clearly lower for the thinnest films.

In addition, a study of temperature dependence of the resistivity has been realized on the various magnetite layers. We observe four orders of magnitude drop between the film resistance at 60 K and at 300 K and obtain a resistivity of the order of  $10^{-3} \Omega \text{ cm}$  at room temperature. However we do not observe a discontinuity in the resistivity around 100–120 K temperature range corresponding to the Verwey transition [17]. The absence of Verwey transitions in thin films has already been reported by several authors [11,16,18] and explained by Mott [17] by the blocking of the Fe<sup>2+</sup>/Fe<sup>3+</sup> fluctuations by impurities. More recently, Garcia *et al.* [19] give an alternative dis-

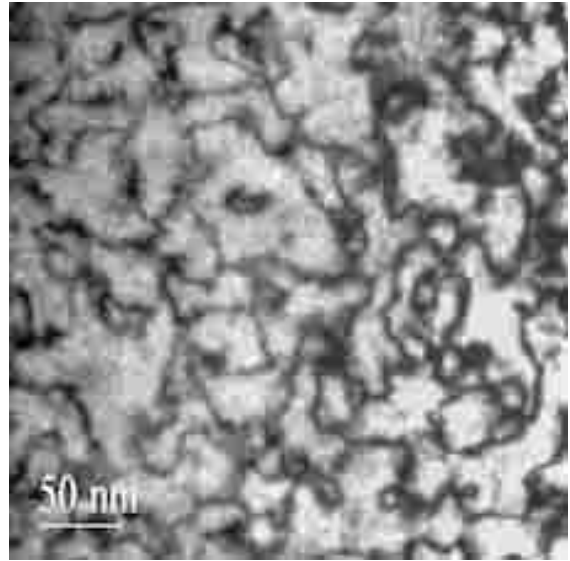


**Fig. 6.** 220 dark field image of a 750 Å thick Fe<sub>3</sub>O<sub>4</sub> film studied in plane view. The dark diffuse contrast corresponds to the APBs.

cussion of the origin of the Verwey transition related to the oxygen sites condensation. In all cases, this cannot exclude the magnetite nature of our films.

## 4 Observation of antiphase boundaries and magnetic domains

### 4.1 TEM observations

TEM analyses were performed on plane view and cross sectional specimen to study the appearance and the morphology of APBs. In Figure 6 is reported a 220 dark field image obtained on a plane view sample of a 750 Å thick Fe<sub>3</sub>O<sub>4</sub> thin film. The diffuse dark contrast corresponds to the APBs across which the {220} planes are discontinuous. These boundaries have a very low energy and then no particular orientation. Consequently, they may be twisted and oriented in all the directions of the crystal. The diffuse aspect of these APBs and their apparent width visible on the dark field images come from the superimposition of the boundaries through the total thickness of the thin TEM specimen. These APBs surround regions whose diameters are about 300 to 500 Å. TEM dark field experiments were also performed on the same 750 Å thick Fe<sub>3</sub>O<sub>4</sub> film studied in cross section. As observed on the 202 dark field micrograph in Figure 7, most of the APBs are elongated perpendicular to the Fe<sub>3</sub>O<sub>4</sub>/MgO interface. This particular APBs orientation may be due to the misfit dislocations and/or to the presence of any defects like steps at the MgO surface. A step at the MgO surface will indeed induce a stacking fault of the magnetite structure growing upon it and a misfit dislocation will create a local strain field in

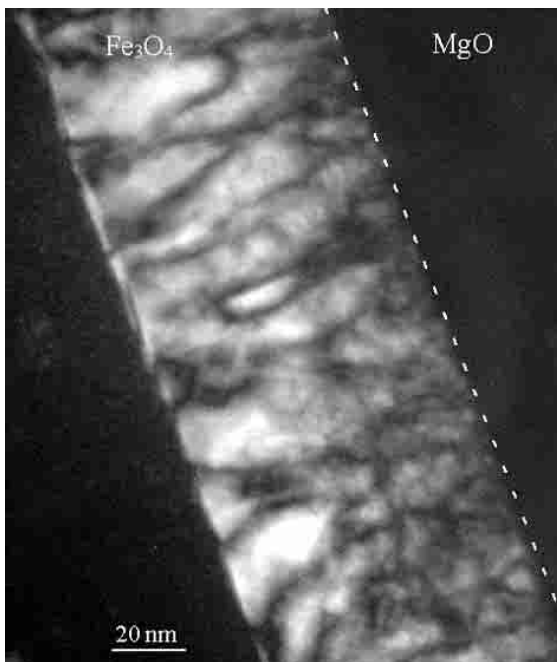


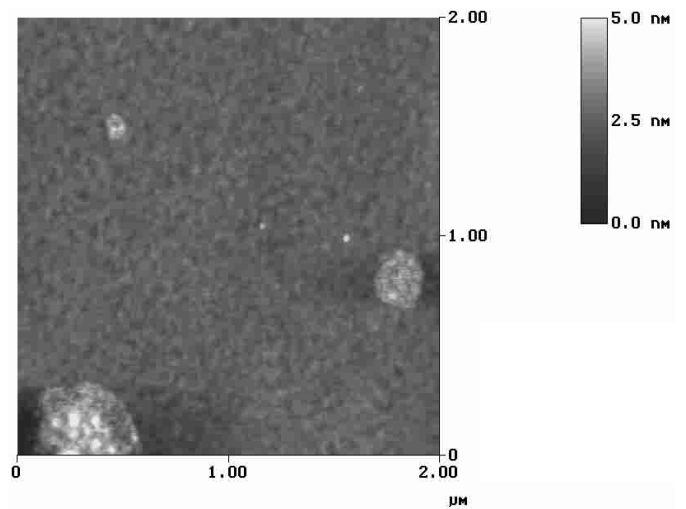
**Fig. 7.** 202 dark field image of a 750 Å thick  $\text{Fe}_3\text{O}_4$  film studied in cross section. Note that APBs are mainly oriented perpendicular to the interface.

the magnetite film that may be a preferential place for the APBs to grow. Both defects could then favor the localization of the APBs at the  $\text{Fe}_3\text{O}_4/\text{MgO}$  interface which will therefore propagate perpendicular to this interface as it is observed in the dark field image in Figure 7.

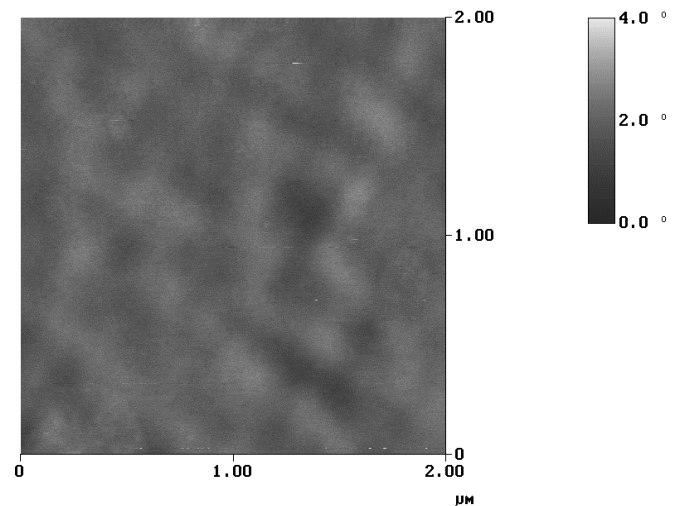
#### 4.2 Domain structure investigations by MFM

The domain structure has been observed in zero field for magnetite layers of different thicknesses. We used a Nanoscope III equipped with a CoCr coated Si tip. The microscope tip was scanning both in tapping mode for the surface morphology and in lift mode for magnetic domain boundary detection 50 nm above the surface. Surface morphology agrees with HRTEM and RHEED data, evidencing a smooth surface with a residual roughness lower than 5 nm peak to peak (see Fig. 8a). The feature size of the surface morphology is close to the APBs spacing observed by TEM ( $\sim 500$  Å).

The typical magnetic structure presented in Figure 8b reveals a domain size roughly 10 times larger than the size of the morphological details. For the three different samples studied, the mean magnetic ripple periodicity is respectively 2000 Å, 2500 Å and 6000 Å for film thickness of 95 Å, 750 Å and 1875 Å. As shown by TEM, the APBs spacing increases with the film thickness, thus there is a correlation between APBs periodicity and magnetic ripple. One more striking feature is the orientation of the



(a)



(b)

**Fig. 8.** Atomic (a) and magnetic (b) force microscopy images of a 750 Å thick  $\text{Fe}_3\text{O}_4$  film.

magnetic ripple as observed in Figure 8b (the  $x$  and  $y$  axes of the AFM/MFM image are  $[100]$  and  $[010]$  crystallographic directions). The magnetic domain boundaries are mostly oriented along  $\{110\}$  planes. This is strongly suggestive that the boundaries planes of  $\{110\}$  family mainly contribute to the antiferromagnetic coupling between adjacent magnetite domains and that  $\{100\}$  type APBs play a minor role. However, since the ripple periodicity is 10 times larger than the APBs periodicity we assume that only a few of the latter induce sufficient antiferromagnetic interactions for obtaining a local magnetization reversal. Clearly, in the MFM measurements, reciprocal effects are present and the stray field generated

by the tip could, in his turn, influence the magnetic structure of the film. All the problem depends of the stray field intensity compared to the anisotropy field of the film (see Ref. [20] for example). For the magnetite films studied in the present work, the coercivity is close to 300 Oe, therefore larger than the stray field of the tip which is made of non magnetic material coated by a CoCr alloy.

This observation allows us to propose that most of the APBs do not induce separate opposite magnetic regions. As explained by Margulies *et al.* [12] there are various types of APBs involving different exchange interactions, and also several configurations with the interplay of more than 2 adjacent domains. These remarks agree with the fact that, in applied fields of 5 T, only 20% of the magnetization remains pinned by antiferromagnetic interactions through APBs.

## 5 Conclusion

Using sputtering technique, we have prepared epitaxial magnetite layers. In particular we observe by HREM that Fe<sub>3</sub>O<sub>4</sub> grows epitaxially on MgO (001) single crystal and that the interface presents very few defects which is one of the requirements for tunneling current with spin polarized carriers. Mössbauer experiments have demonstrated that we have a correct distribution of the Fe cations in two different oxidation states as in bulk Fe<sub>3</sub>O<sub>4</sub> inverse spinel, A sites contain only Fe<sup>3+</sup> ions and the B sites contain equal numbers of Fe<sup>2+</sup> and Fe<sup>3+</sup> ions. Polar Kerr spectra show a good agreement with bulk Fe<sub>3</sub>O<sub>4</sub> tabulated spectra.

The main structural defects found in our samples are antiphase boundaries (APBs). TEM studies of these APBs show that they are mostly oriented perpendicular to the film. MFM reveals a magnetic ripple that is correlated to the presence of APBs but with a larger lengthscale, suggestive that a fraction of the APBs, more particularly the ones oriented along {110} planes, contribute to the magnetic properties. All these results evidence the strong interest to develop heterostructures for spin dependent transport with thin Fe<sub>3</sub>O<sub>4</sub> films, provided the possibility to reduce the APBs density which causes a low squareness of their magnetization loops.

## References

1. R.J. Soulen, J.M. Byers, M.S. Osofsky, B. Nadgorny, T. Ambrose, S.F. Cheng, P.R. Broussard, C.T. Tanaka, J. Novwak, J.S. Moodera, A. Barry, J.M.D. Coey, *Science* **282**, 85 (1998).
2. Kobayashi *et al.*, *Nature* **395**, 677 (1998).
3. B.D. Cullity, *Introduction to Magnetic Materials* (Addison-Wesley, Reading, MA, 1972).
4. Z. Zang, K. Satpathi, *Phys. Rev. B* **44**, 13319 (1991).
5. A. Yanase, K. Siratori, *J. Phys. Soc. Jpn* **53**, 132 (1984).
6. P. Seneor, A. Fert, J.L. Maurice, F. Petroff, A. Vaurès, *Appl. Phys. Lett.* **74**, 4017 (1999).
7. X.W. Li, A. Gupta, Gang Xiao, W. Qian, V.P. Dravid, *Appl. Phys. Lett.* **73**, 3282 (1998).
8. J.M.D. Coey, A.E. Berkowitz, Ll. Balcells, F.F. Putris, F.T. Parker, *Appl. Phys. Lett.* **72**, 734 (1998).
9. K. Ghosh, S.B. Ogale, S.P. Pai, M. Robson, E. Li, I. Jin, Ziwen Dong, R.L. Greene, R. Ramesh, T. Venkatesan, *Appl. Phys. Lett.* **73**, 689 (1998).
10. G.Q. Gong, A. Gupta, Gang Xiao, W. Qian, V.P. Dravid, *Phys. Rev. B* **56**, 5096 (1997).
11. D.T. Margulies, F.T. Parker, F.E. Spada, R.S. Goldman, J. Li, R. Sinclair, A.E. Berkowitz, *Phys. Rev. B* **53**, 9175 (1996).
12. D.T. Margulies, F.T. Parker, M.L. Rudee, F.E. Spada, J.N. Chapman, P.R. Aitchison, A.E. Berkowitz, *Phys. Rev. Lett.* **79**, 5162 (1997).
13. J.F. Bobo, S. Dubourg, E. Snoeck, B. Warot, P. Baules, J.C. Ousset, *J. Magn. Magn. Mater.* **206**, 118 (99).
14. W.F.J. Fontijn, P.J. van der Zaag, M.A.C. Devillers, V.A.M. Brabers, R. Metselaar, *Phys. Rev. B* **56**, 5432 (1997).
15. W. F.J. Fontijn, P.J. van der Zaag, R. Metselaar, *J. Appl. Phys.* **83**, 6765 (1998).
16. S.B. Ogale, K. Ghosh, R.P. Sharma, R.L. Greene, R. Ramesh, T. Venkatesan, *Phys. Rev. B* **57**, 7823 (1998).
17. *Metal Insulator Transitions*, edited by N.F. Mott (Taylor and Francis, 1990), p. 215.
18. X.W. Li, G.Q.A. Gupta, G. Xiao, *J. Appl. Phys.* **83**, 734 (1998).
19. J. Garcia, G. Subias, M.G. Proietti, J. Blasco, H. Renevier, J.L. Hodeau, Y. Joly, *Phys. Rev. B* **63**, 054110 (2001).
20. U. Hartmann, *Phys. Stat. Sol. (a)* **115**, 285 (1989).